

Burst-by-Burst Adaptive Decision Feedback Equalized TCM, TTCM, and BICM for H.263-Assisted Wireless Video Telephony

Soon Xin Ng, Jin Yee Chung, Peter Cherriman, and Lajos Hanzo

Abstract—Decision feedback equalizer-aided wide-band burst-by-burst adaptive trellis-coded modulation, turbo trellis-coded modulation (TTCM), and bit-interleaved-coded modulation-assisted H.263-based video transceivers are proposed and characterized in performance terms when communicating over the COST 207 typical urban wide-band fading channel. Specifically, four different modulation modes, namely 4QAM, 8PSK, 16QAM, and 64QAM are invoked and protected by the above-mentioned coded modulation schemes. The TTCM assisted scheme was found to provide the best video performance, although at the cost of the highest complexity. A range of lower-complexity arrangements will also be characterized. Finally, in order to confirm these findings in an important practical environment, we have also investigated the adaptive TTCM scheme in the CDMA-based universal mobile telecommunications systems terrestrial radio access (UTRA) scenario and the good performance of adaptive TTCM scheme recorded when communicating over the COST 207 channels was retained in the UTRA environment.

Index Terms—Adaptive CDMA, adaptive quadrature amplitude modulation (AQAM), bit-interleaved-coded modulation (BICM), coded modulation (CM), decision feedback equalizer (DFE), H.263, joint decision (JD), peak signal-to-noise ratio (PSNR), trellis-coded modulation (TCM), turbo trellis-coded modulation (TTCM), video telephony, universal mobile telecommunications system (UMTS) terrestrial radio access (UTRA).

I. INTRODUCTION

M -ary coded modulation (CM) schemes such as trellis-coded modulation (TCM) [1] and bit-interleaved-coded modulation (BICM) [2], [3] constitute powerful and bandwidth efficient forward error correction schemes, which combine the functions of coding and modulation. It was found in [2] and [3] that BICM is superior to TCM when communicating over narrowband Rayleigh fading channels, but inferior to TCM in Gaussian channels. In 1993, power efficient binary turbo convolutional codes (TCCs) were introduced in [4], which are capable of achieving a low bit-error rate at low signal-to-noise ratios (SNR). However, TCCs typically operate at a fixed coding rate of 1/2 and they were originally designed

for binary-phase-shift-keying (BPSK) modulation, hence, they require doubling the bandwidth. In order to lend TCCs a higher spectral efficiency, BICM using TCCs was first proposed in [5], where it was also referred to as turbo-coded modulation (TuCM). As another design alternative, turbo trellis-coded modulation (TTCM) was proposed in [6], which has a structure similar to that of the family of TCCs, but employs TCM codes as component codes. It was shown in [6] that TTCM performs better than TCM and TuCM at a comparable complexity. Many other bandwidth efficient schemes using turbo codes, such as multilevel coding employing turbo codes [7], have been proposed in the literature [8], but here we focus our study on the family of TCM, BICM, and TTCM schemes in the context of a wireless video telephony system.

In general, fixed-mode transceivers fail to adequately accommodate and counteract the time varying nature of the mobile radio channel. Hence, their error distribution becomes bursty and this would degrade the performance of most channel coding schemes, unless long-delay channel interleavers are invoked. However, the disadvantage of long-delay interleavers is that owing to their increased latency they impair “lip-synchronization” between the voice and video signals. By contrast, in burst-by-burst (BbB) adaptive quadrature amplitude (or phase shift keying) modulation (AQAM) schemes [9]–[21] a higher order modulation mode is employed, when the instantaneous estimated channel quality is high for the sake of increasing the number of bits per symbol (BPS) transmitted. Conversely, a more robust but lower-throughput modulation mode is used, when the instantaneous channel quality is low, in order to improve the mean bit-error ratio (BER) performance. Uncoded AQAM schemes [10]–[13] and channel-coded AQAM schemes [14]–[20] have been lavishly investigated in the context of narrowband fading channels. In particular, adaptive trellis-coded M -ary PSK was considered in [14] and coset codes were applied to adaptive trellis-coded M -ary QAM in [16]. *However, these contributions were based on a number of ideal assumptions, such as perfect channel estimation and zero modulation mode feedback delay.* Hence, in [17], adaptive TCM using more realistic outdated fading estimates was investigated. Recently, the performance of adaptive TCM based on realistic practical considerations such as imperfect channel estimation, modem mode signalling errors and modem mode feedback delay was evaluated in [18], where the adaptive TCM scheme was found to be robust in most practical situations, when communicating over narrowband fading channels. In an effort to increasing the so-called time-diversity order of the TCM codes, adaptive BICM schemes have been

Manuscript received December 1, 2004; revised June 2, 2005. This work was supported in part by the Engineering and Physical Science Research Council, U.K., and the European Union under the auspices of the PHOENIX and NEWCOM projects. This paper was recommended by Associate Editor C. Guillemot.

S. X. Ng, P. Cherriman, and L. Hanzo are with the School of Electrical and Computer Science, University of Southampton, SO17 1BJ, U.K. (e-mail: lh@ecs.soton.ac.uk).

J.Y. Chung is with Frontier Silicon Ltd., Cambridge CB2 4LJ, U.K.
Digital Object Identifier 10.1109/TCSVT.2006.869968

proposed in [19], although their employment was still limited to communications over narrowband fading channels.

On the other hand, for communications over wide-band fading channels, a BbB adaptive transceiver employing separate channel coding and modulation schemes was proposed in [22]. The main advantage of this wide-band BbB adaptive scheme is that regardless of the prevailing channel conditions, the transceiver achieves always the best possible source-signal representation quality such as video, speech, or audio quality by automatically adjusting the achievable bit rate and the associated multimedia source-signal representation quality in order to match the channel quality experienced. Specifically, this wide-band BbB adaptive scheme employs the adaptive video rate control and packetization algorithm of [23], which generates exactly the required number of video bits for the channel-quality-controlled BbB adaptive transceiver, depending on the instantaneous modem-mode-dependent payload of the current packet, as determined by the current modem mode. Hence, a channel-quality-dependent variable-sized video packet is transmitted in each time division multiple access (TDMA) frame constituted by a fixed number of AQAM symbols and, hence, the best possible source-signal representation quality is achieved on a near-instantaneous basis under given propagation conditions in order to cater for the effects of path-loss, fast-fading, slow-fading, dispersion, co-channel interference, etc. More explicitly, a half-rate Bose–Chaudhuri–Hocquenghem (BCH) block code and a half-rate TCC were employed and the modulation modes were adapted according to the channel conditions. However, due to the fixed coding rate of the system the range of the effective video bit rates was limited. Hence, in this contribution our objective is to further develop the wireless video telephone system of [22] by increasing its bandwidth efficiency up to a factor of two upon rendering not only the modulation-mode selection, but also the choice of the channel coding rate near instantaneously adaptive with the advent of the aforementioned bandwidth efficient CM schemes. As a second objective, we extend this adaptive CM philosophy to multiuser scenarios in the context of a UMTS terrestrial radio access (UTRA) [24], [25] system.

The paper is organized as follows. In Section II the systems architecture is outlined. In Section III, the performance of various fixed-mode CM schemes is characterized, while in Section IV the performance of adaptive CM schemes is evaluated. In Section V the performance of the adaptive TCC based video system is studied in the UTRA CDMA environment. Finally, we will conclude in Section VI.

II. SYSTEM OVERVIEW

The simplified block diagram of the BbB adaptive CM scheme is shown in Fig. 1, where channel interleaving spanning

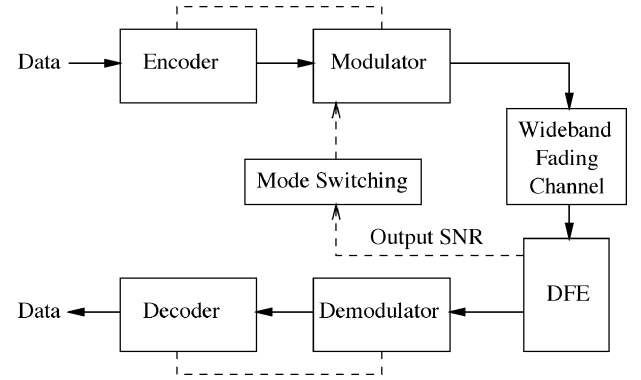


Fig. 1. Block diagram of the BbB adaptive CM scheme.

one transmission burst is used. The length of the CM codeword is one transmission burst. We invoke four CM encoders for our quadruple-mode adaptive CM scheme, each attaching one parity bit to each information symbol generated by the video encoder, yielding a channel coding rate of 1/2 in conjunction with the modulation modes of 4QAM, a rate of 2/3 for 8PSK, 3/4 for 16QAM, and 5/6 for 64QAM. The complexity of the CM schemes is compared in terms of the number of decoding states and the number of decoding iterations. For a TCM or BICM code of memory M , the corresponding complexity is proportional to the number of decoding states $S = 2^M$. Since TCCM schemes invoke two component TCM codes, a TCCM code employing t iterations and using an S -state component code exhibits a complexity proportional to $2.t.S$ or $t.2^{M+1}$.

Over wide-band fading channels, the employed minimum mean squared error (MMSE)-based decision feedback equalizer (DFE) eliminates most of the channel-induced intersymbol interference (ISI). Consequently, the mean-squared error at the output of the DFE can be calculated and used as the channel quality metric invoked for switching the modulation modes. More explicitly, the residual signal deviation from the error-free transmitted phasors at the DFEs output reflects the instantaneous channel quality of the time varying wide-band fading channel. Hence, given a certain instantaneous channel quality, the most appropriate modulation mode can be chosen according to this residual signal deviation from the error-free transmitted phasors at the DFEs output. Specifically, the SNR at the output of the DFE γ_{dfe} can be computed as [13] (1), shown in the equation at the bottom of the page, where C_m and h_m denote the DFEs feed-forward coefficients and the channel impulse response (CIR), respectively. The transmitted signal represented by s_k and N_0 denotes the noise spectral density. Finally, the number of DFE feed-forward coefficients is denoted by N_f . The equalizers output SNR γ_{dfe} in (1), is then compared against a set of adaptive modem mode switching

$$\gamma_{dfe} = \frac{\text{Wanted Signal Power}}{\text{Residual ISI Power} + \text{Effective Noise Power}} = \frac{E \left[\left| s_k \sum_{m=0}^{N_f} C_m h_m \right|^2 \right]}{\sum_{q=-(N_f-1)}^{-1} E \left[\left| \sum_{m=0}^{N_f-1} C_m h_{m+q} s_{k-q} \right|^2 \right] + N_0 \sum_{m=0}^{N_f} |C_m|^2} \quad (1)$$

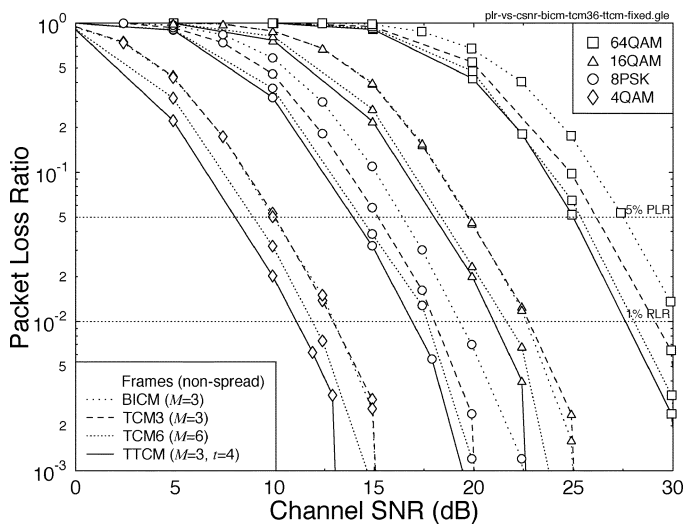


Fig. 2. Packet loss ratio versus channel SNR for the four fixed modem modes, using the four joint coding/modulation schemes considered, namely BICM, TCM3, TCM6, and TTCM when communicating over the COST 207 channel [28].

thresholds f_n , and subsequently the appropriate modulation mode is selected [13].

In the adaptive transmission schemes, the outdated channel quality estimates arriving after a feedback delay inevitably inflict performance degradations, which can be mitigated using powerful channel quality prediction techniques [26], [27]. However, in our proposed adaptive video system, we adopted the practical approach of employing outdated, rather than perfect, channel quality estimates. Specifically, a practical modem mode switching regime adapted to the specific requirements of wireless video telephony is employed, where a suitable modulation mode is chosen at the receiver on a BbB basis and it is then communicated to the transmitter by superimposing the requested modulation mode identifier code onto the terminals reverse-direction transmission burst. Hence, the actual channel condition is outdated by one TDMA/TDD frame duration.

At the receiver, the DFEs symbol estimate \hat{s}_k is passed to the channel decoder and the log-maximum domain branch metric is computed for the sake of maximum-likelihood decoding at time instant k as

$$m_k(s_i) = -\frac{|\hat{s}_k - s_i|^2}{2\sigma^2}, \quad i = \{0, \dots, \mathcal{M} - 1\} \quad (2)$$

where s_i is the i th legitimate symbol of the \mathcal{M} -ary modulation scheme and σ^2 is the variance of the additive white gaussian noise (AWGN). Note that the equalizer output \hat{s}_k is near-Gaussian, since the channel has been equalized [13]. In other words, the DFE has “converted” the dispersive Rayleigh fading channels into an “AWGN-like” channel. Hence, the TCM and TTCM codes that have been designed for AWGN channels will outperform the BICM scheme, as we will demonstrate in Fig. 2.

The following assumptions are stipulated. First, we assume that the equalizer is capable of estimating the CIR perfectly with the aid of the equalizer training sequence hosted by the transmission burst of Fig. 3. Second, the CIR is time-invariant for the

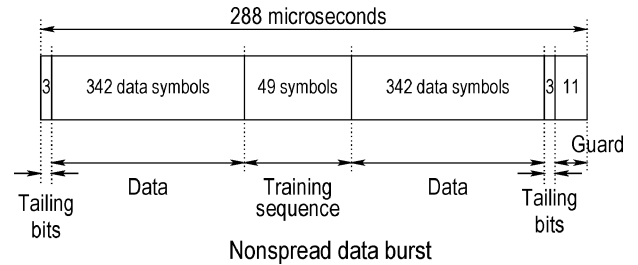


Fig. 3. Transmission burst structure of the FMA1 nonspread data as specified in the FRAMES proposal [29].

TABLE I
OPERATIONAL-MODE SPECIFIC TRANSCIEVER PARAMETERS FOR TTCM

Features	Multi-rate System			
	4QAM	8PSK	16QAM	64QAM
Mode	4QAM	8PSK	16QAM	64QAM
Transmission Symbols/TDMA slot	684			
Bits/Symbol	2	3	4	6
Transmission bits/TDMA slot	1368	2052	2736	4104
Packet Rate	216.7/s			
Transmission bitrate (kbit/s)	296.4	444.6	592.8	889.3
Code Termination Symbols	6			
Data Symbols/TDMA slot	678			
Coding Rate	1/2	2/3	3/4	5/6
Information Bits/Symbol	1	2	3	5
Unprotected bits/TDMA slot	678	1356	2034	3390
Unprotected bitrate (kbit/s)	146.9	293.8	440.7	734.6
Video packet CRC (bits)	16			
Feedback protection (bits)	9			
Video packet header (bits)	11	12	12	13
Video bits/packet	642	1319	1997	3352
Effective Video-rate (kbit/s)	139.1	285.8	432.7	726.3
Video framerate (Hz)	30			

duration of a transmission burst, but varies from burst to burst according to the Doppler frequency, which corresponds to assuming that the CIR is slowly varying.

A. System Parameters and Channel Model

For the sake of direct comparisons, we used the same H.263 video codec, as in [22]. Hence, we refer the interested readers to [24] for a detailed description of the H.263 video codec. The transmitted bit rate of all four modes of operation is shown in Table I for the TTCM coding scheme. The associated bit rates are similar for the other CM schemes. The slight difference is caused by using different numbers of code termination symbols. The unprotected bit rate before channel coding is also shown in the table. The actual useful bit rate available for video encoding is slightly lower, than the unprotected bit rate due to the useful bit rate reduction required by the transmission of the strongly protected packet acknowledgment information and packetization overhead information. The effective video bit rate is also shown in the table, which varies from 139 to 726 kb/s. We have investigated the video system concerned using a wide range of

TABLE II
MODULATION AND CHANNEL PARAMETERS

Parameter	Value
Carrier Frequency	1.9GHz
Vehicular Speed	30mph
Doppler frequency	85Hz
Normalised Doppler frequency	3.3×10^{-5}
Channel type	COST 207 Typical Urban [28]
Number of paths in channel	4
Data modulation	Adaptive Coded Modulation (4-QAM, 8-PSK, 16-QAM, 64-QAM)
Receiver type	Decision Feedback Equalizer Number of Forward Filter Taps = 35 Number of Backward Filter Taps = 7

video sequences having different resolutions. However for conciseness we will only show results for the CIF resolution (352 × 288 pixels) “Salesman” sequence at 30 frames/s.

Table II shows the modulation and channel parameters employed. Again, similar to [22], the COST 207 [28] channel models, which are widely used in the community, were employed. Specifically, a 4-path Typical Urban COST 207 channel [28] was used. The multipath channel model is characterized by its discretized symbol-spaced CIR, where each path is faded independently according to a Rayleigh distribution. The nonspread data transmission burst structure FMA1 specified in the FRAMES proposal [29] was used, which is shown in Fig. 2. Nyquist signalling was employed and the remaining system parameters are shown in Table III. A component TCM having a code memory of $M = 3$ was used for the TTCM scheme. The number of iterations for TTCM was fixed to $t = 4$ and, hence, the iterative scheme exhibited a similar decoding complexity to that of the TCM having a code memory $M = 6$ in terms of the number of coding states. The fixed-mode CM schemes that we invoked in our BbB AQAM schemes are Ungerböcks TCM [1], [30], Robertsons TTCM [6], [30], and Zehavis BICM [2], [30]. Soft decision trellis decoding utilising the log-maximum *a posteriori* algorithm [31] was invoked for decoding.

Note that the parameters of the DFE employed, which are the same as that of [22], as well as that of the joint detection (JD) receiver in Section V were adjusted such that they achieve their best attainable performance in terms of removing the effect of channel induced multipath interference as well as the multiuser interference, respectively. Hence, opting for a more complex DFE or JD design would not improve the overall achievable performance. Furthermore, since the video quality expressed in terms of the luminance peak SNR (PSNR) is a direct function of the systems effective throughput, we will use the PSNR value as the ultimate evaluation metric of the systems performance. Since the same video system and channel model are employed, the complexity difference between the various CM-assisted video schemes is directly dependent on the decoding complexity of the CM schemes. Hence, the complexity of the proposed video system is estimated in terms of the number of trellis states of the CM decoders.

TABLE III
GENERIC SYSTEM FEATURES OF THE RECONFIGURABLE MULTI-MODE VIDEO TRANSCIVER, USING THE NON-SPREAD DATA BURST MODE OF THE FRAMES PROPOSAL [29] SHOWN IN FIG. 3

Features	Value
Multiple access	TDMA
No. of Slots/Frame	16
TDMA frame length	4.615ms
TDMA slot length	288 μ s
Data Symbols/TDMA slot	684
User Data Symbol Rate (kBd)	148.2
System Data Symbol Rate (MBd)	2.37
Symbols/TDMA slot	750
User Symbol Rate (kBd)	162.5
System Symbol Rate (MBd)	2.6
System Bandwidth (MHz)	3.9
Eff. User Bandwidth (kHz)	244

III. EMPLOYING FIXED MODULATION MODES

Initial simulations of the videophone transceiver were performed with the transceiver configured in one of the four fixed modulation modes of Table I. We commence by comparing the performance of TTCM in conjunction with a code memory of $M = 3$ and using $t = 4$ iterations, to that of noniterative TCM along with a code memory of $M = 6$, since the associated computational complexity is similar. We then also compare these results to that of TCM using a code memory of $M = 3$ and to BICM employing a code memory $M = 3$. Again, one video packet is transmitted in each TDMA frame and the receiver checks, whether the received packet has any bit errors using the associated cyclic redundancy check (CRC). If the received packet has been corrupted, a negative acknowledgment flag is transmitted to the video encoder in order to prevent it from using the packet just transmitted for updating the encoders reconstruction frame buffer. This allows the video encoders and decoders reconstruction frame buffer to use the same contents for motion compensation. This acknowledgment message is strongly protected using repetition codes and superimposed on the reverse link transmission. In these investigations a transmission frame error resulted in a video packet error. We shall characterize the relative frequency of these packet corruption events by the packet loss ratio (PLR). The PLR of the CM schemes is shown in Fig. 2. We emphasise again that the video packets are either error-free or discarded. Hence, the PLR is a more meaningful modem performance metric in this scenario, than the BER.

From Fig. 2, it is found that the BICM scheme has the worst PLR performance and the TCM6 scheme using a code memory $M = 6$ has a significant PLR performance advantage over the TCM3 scheme employing a code memory of $M = 3$. Furthermore, the TTCM scheme provides the best PLR performance, requiring an approximately 2.5 dB lower channel SNR than the

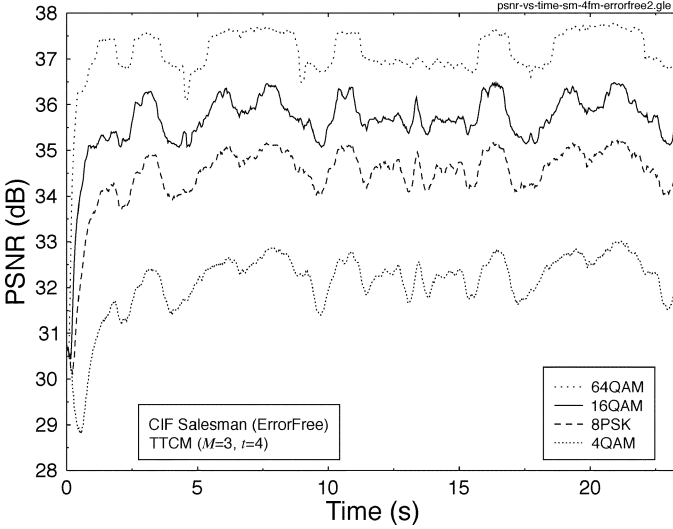


Fig. 4. PSNR (video quality) versus time for the four modulation modes, under error-free channel conditions using the CIF resolution “Salesman” video sequence at 30 frame/s. TTCM scheme using a code memory of $M = 3$ and $t = 4$ iterations was employed.

BICM scheme. This is because turbo decoding of the TTCM scheme is very effective in reducing the number of bit errors to zero in all the received packets exhibiting a moderate or low number of bit errors before channel decoding. By contrast, the gravely error-infected received packets are simply dropped and the corresponding video frame segment is replaced by the same segment of the previous frame. The performance of BICM is worse, than that of TCM due to the associated limited channel interleaving depth [2], [3] of the BICM scheme in our slow-fading wide-band channels.

Fig. 4 shows the error-free decoded video quality, measured in terms of the PSNR versus time for the CIF-resolution “Salesman” sequence for each of the four fixed modulation modes using the TTCM scheme. The figure demonstrates that the higher order modulation modes, which have a higher associated bit rate provide a better video quality. However, in an error-impaired situation a high error-free PSNR does not always guarantee achieving a better subjective video quality. In order to reduce the detrimental effects of channel-induced errors on the video quality, we refrain from decoding the error-infested video packets and, hence, avoid error propagation through the reconstructed video frame buffer [22], [23]. Instead, these originally high-bit rate and high-quality but error-infested video packets are dropped and, hence, the reconstructed video frame buffer will not be updated, until the next packet replenishing the specific video frame area arrives. As a result, the associated video performance degradation becomes fairly minor for PLR values below 5% [22], which is significantly lower than in case of replenishing the corresponding video frame area with the error-infested video packet.

IV. EMPLOYING ADAPTIVE MODULATION

The BbB AQAM mode switching mechanism is characterized by a set of switching thresholds, by the corresponding random TTCM symbol-interleavers and the component codes,

TABLE IV
SWITCHING THRESHOLDS ACCORDING TO EQUATION (3) AT THE OUTPUT OF THE EQUALIZER REQUIRED FOR EACH MODULATION MODE OF THE BbB ADAPTIVE MODEM. THE THRESHOLD TYPES ARE NORMAL (N), CONSERVATIVE (C) AND AGGRESSIVE (A). M DENOTES THE CODE MEMORY OF THE ENCODER

No.	Scheme	M	Type	Thresholds (dB)		
				f_1	f_2	f_3
1.	TTCM	3	N	13.07	17.48	24.77
2.	TTCM	3	C	16.00	20.00	27.25
3.	TTCM	3	A	10.05	12.92	20.67
4.	TCM	3	N	14.48	18.86	26.24
5.	TCM	6	N	13.98	17.59	25.37
6.	BICM	3	N	15.29	18.88	26.49

as follows:

Modulation Mode

$$= \begin{cases} 4\text{QAM}, I_0 = I_s, R_0 = \frac{1}{2}, & \text{if } \gamma_{\text{DFE}} \leq f_1 \\ 8\text{PSK}, I_1 = 2I_s, R_1 = \frac{2}{3}, & \text{if } f_1 < \gamma_{\text{DFE}} \leq f_2 \\ 16\text{QAM}, I_2 = 3I_s, R_2 = \frac{3}{4}, & \text{if } f_2 < \gamma_{\text{DFE}} \leq f_3 \\ 64\text{QAM}, I_3 = 5I_s, R_3 = \frac{5}{6}, & \text{if } \gamma_{\text{DFE}} > f_3 \end{cases} \quad (3)$$

where $f_n, n = 1, \dots, 3$ are the AQAM switching thresholds, which were set according to the target PLR requirements, while $I_s = 684$ is the number of data symbols in a transmission burst and I_n represents the random TTCM symbol-interleaver size expressed in terms of the number of bits, which is not used for the TCM and BICM schemes.

The video encoder/decoder pair discards all corrupted video packets in an effort to avoid error propagation effects in the video decoder. Therefore, in this contribution the AQAM switching thresholds f_n were chosen using an experimental procedure in order to maintain the required target PLR, rather than the BER. More specifically, we defined a set of “normal” thresholds for each adaptive CM scheme depending on their fixed modem modes performance in terms of PLR versus average equalizer SNR. Explicitly, the “normal” threshold was set to maintain a PLR around 3%. We also defined a “conservative” threshold, for a PLR around 0.5%, and an “aggressive” threshold, for a PLR around 20% for the adaptive TTCM scheme. These modem mode switching thresholds are listed in Table IV.

The probability density function (pdf) of each of the modulation modes versus channel SNR is shown in Fig. 5 for the BbB adaptive TTCM scheme using the “normal” switching thresholds. The graph shows that the 4QAM mode is the most probable one at low channel SNRs, and the 64QAM mode is predominant at high channel SNRs. In addition, for example at 20 dB, the 4QAM mode is being used about 8% of the time, and 64QAM only 1% of the time, since most of the time the AQAM modem is operating in its 8PSK or 16QAM mode with an associated probability of 40% and 51%, respectively.

A. Performance of TTCM AQAM

In this section, we compare the performance of the four fixed modulation modes with that of the quadruple-mode TTCM AQAM scheme using the “normal” switching thresholds of

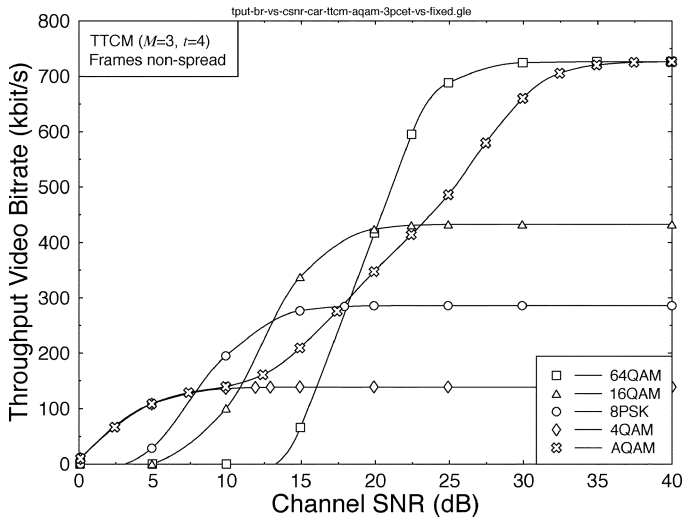


Fig. 7. Throughput video bit rate versus channel SNR for the four fixed-modes and for the quadruple-mode TTCM AQAM scheme using the “normal” thresholds of Table IV, employing a code memory of $M = 3$ and $t = 4$ iterations when communicating over the COST 207 channel of [28].

Table IV. The code memory is $M = 3$ and the number of turbo iterations is $t = 4$.

Specifically, in Fig. 6, we compare the PLR performance of the four fixed modulation modes with that of the quadruple-mode TTCM AQAM arrangement using the “normal” switching thresholds. The figure shows that the performance at low channel SNRs is similar to that of the fixed TTCM 4QAM mode, while at high channel SNRs the performance is similar to that of the fixed 64QAM mode. At medium SNR values the PLR performance is near-constant, ranging from 1% to 5%. More explicitly, the TTCM AQAM modem maintains this near-constant PLR, which is higher than that of the fixed 4QAM modem, while achieving a higher throughput bit rate, than the 2 bit/symbol rate of 4QAM. Since our BbB AQAM videophone systems video performance is closely related to the PLR, the TTCM AQAM scheme provides a near-constant video performance across a wide range of channel SNRs. Additionally, the BbB TTCM AQAM modem allows the throughput bit rate to increase, as the channel SNR increases, thereby supporting an improved video quality, as the channel SNR improves, which is explicitly shown in Fig. 7.

The effective throughput bit rate of the fixed-mode modems drops rapidly due to the increased PLR, which is a consequence of discarding the “payload” of the corrupted video packets, as the channel SNR reduces. The TTCM AQAM throughput bit rate matches that achieved by the fixed modem modes at both low and high channel SNRs. At a channel SNR of 25 dB the fixed-mode 64QAM modem achieves an approximately 700 kbps throughput, while the TTCM AQAM modem transmits at approximately 500 kbps. However, by referring to Fig. 6 it can be seen that the 700 kbps video throughput bit rate is achieved by 64QAM at a concomitant PLR of slightly over 5%, while the AQAM modem experiences a reduced PLR of 2%. As mentioned earlier, the associated video performance degradation becomes noticeable at a PLR in excess of 5%. Hence, the fixed-mode 64QAM modem results in a subjectively inferior video quality in comparison to the TTCM AQAM scheme at a

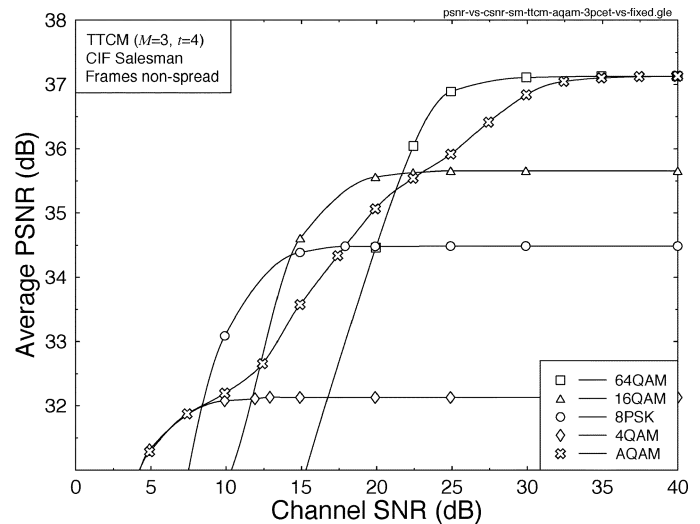


Fig. 8. Average PSNR versus channel SNR for the four fixed TTCM modes and for the quadruple-mode TTCM AQAM scheme, using the “normal” thresholds of Table IV, and the CIF “Salesman” video sequence at 30 frame/s. A code memory of $M = 3$ and $t = 4$ iterations invoked when communicating over the COST 207 channel [28].

channel SNR of 25 dB. The video quality expressed in terms of the average PSNR is closely related to the effective video throughput bit rate. Hence, the trends observed in terms of PSNR in Fig. 8 are similar to those seen in Fig. 7. Note that the channel-quality related AQAM mode feedback is outdated by one TDMA transmission burst of 4.615 ms for the sake of providing realistic results. As shown in [22], in the idealistic zero-delay-feedback AQAM scheme, the resultant PSNR curve follows the envelope of the fixed-mode schemes. However, a suboptimum modulation modes may be chosen due to the one-frame-feedback delay, which may inflict an increased video packet loss. Since the effective throughput is quantified in terms of the average bit rate provided by all the successful transmitted video packets but excluding the erroneous and, hence, dropped packets, the throughput and, hence, the PSNR of the realistic AQAM scheme using outdated channel quality estimates is lower than that of the ideal AQAM scheme. Furthermore, the AQAM systems effective throughput is slightly reduced by allocating some of the useful payload to the AQAM mode signalling information, which is protected by strong repetition coding. Therefore, the throughput or PSNR curve of the AQAM scheme plotted in Figs. 7 or 8 does not strictly follow the throughput or PSNR envelope of the fixed-mode schemes. However, at lower vehicular speeds the switching latency is less crucial and the practical one-frame delay AQAM can achieve a performance that is closer to that of the ideal zero-delay AQAM.

Fig. 8 portrays that the AQAM modems video performance degrades gracefully, as the channel SNR degrades, while the fixed-mode modems’ video performance degrades more rapidly, when the channel SNR becomes insufficient for the reliable operation of the specific modem mode concerned. As we have shown in Fig. 4, the higher order modulation modes, which have a higher associated bit rate provide a higher PSNR in an error-free scenario. However, in the presence of channel errors, the channel-induced PSNR drops and the associated

perceptual video quality degradations imposed by transmission errors are more dramatic when higher order modulation modes are employed. Therefore, annoying video artefacts and a low subjective video perception will be observed when employing higher order modulation modes such as 64QAM during instances of low channel quality. However, these subjective video quality degradations and the associated artefacts are eliminated by the advocated AQAM/TTCM regime, because it operates as a “safety-net” mechanism, which drops the instantaneous AQAM/TTCM throughput in an effort to avoid the dramatic PSNR degradations of the fixed modes during instances of low channel quality, instead of dropping the entire received packet.

B. Performance of AQAM Using TTCM, TCC, TCM and BICM

Let us now compare the video performance of the TTCM-aided AQAM video system to that of the TCC-assisted AQAM video system of [22]. The lowest information throughput of the TTCM AQAM scheme was 1 BPS in the 4QAM mode here, while that of the TCC AQAM scheme of [22] was 0.5 BPS in the BPSK mode. Furthermore, the highest information throughput of the TTCM AQAM scheme was 5 BPS in the 64QAM mode here, while that of the TCC AQAM scheme of [22] was 3 BPS on the 64QAM mode. Hence, we can see from Fig. 7 that TTCM has a video bit rate of about 100 kb/s at SNR = 5 dB and 726 kb/s at SNR = 35 dB. By contrast, the TCC in [22, Fig. 12] has only a video throughput of 50 kb/s at SNR = 5 dB and 409 kb/s at SNR = 35 dB. Hence, we may conclude that at the symbol-rate considered the TTCM scheme has substantially increased the achievable effective video bit rate of the TCC scheme having an identical symbol-rate and characterized in [22]. This increased effective video bit rate allows the TTCM scheme to transmit CIF video frames which are four times larger than the QCIF video frames transmitted by the TCC scheme of [22].

Let us now compare the video performance of the TTCM-aided AQAM video system to that of the TCM- and BICM-assisted AQAM video system. As it was shown in Fig. 3, the TTCM scheme achieved the best PLR performance in a fixed modulation scenario. Therefore, according to Table IV, the AQAM switching thresholds of the TTCM scheme can then be set lower, while still achieving the required PLR performance. The lower thresholds imply that higher order modulation modes can be used at lower channel SNRs and, hence, a higher video transmission bit rate is achieved with respect to the other joint coding and modulation schemes. The PSNR video quality is closely related to the video bit rate. As shown in Fig. 9, the TTCM-based AQAM modem exhibits the highest PSNR video quality followed by the TCM6 scheme having a code memory of $M = 6$, the TCM3 scheme having a code memory of $M = 3$, and finally, the BICM scheme having a code memory of $M = 3$.

As seen in Fig. 9, the PSNR video performance difference of the BICM scheme compared to that of the TTCM scheme is only about 2 dB, since the video quality improvement of TTCM is limited by the moderate turbo interleaver length of our BbB AQAM scheme. Therefore, the low complexity TCM3 scheme provides the best compromise in terms of the PSNR video performance and decoding complexity, since the BICM and TCM3

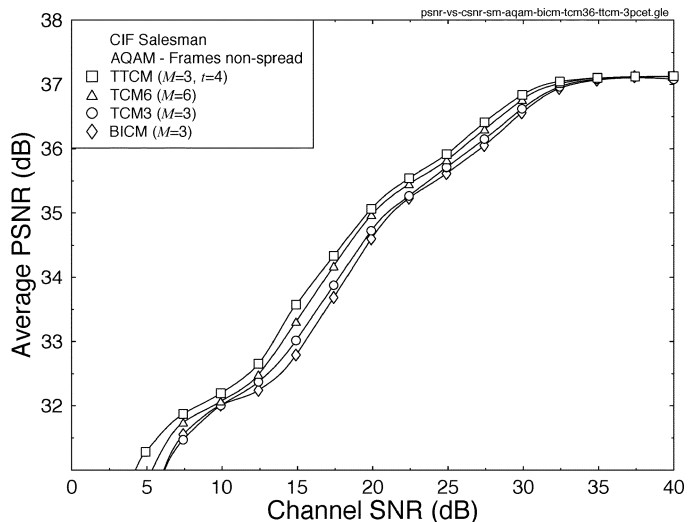


Fig. 9. Average PSNR versus channel SNR for the quadruple-mode AQAM modems using the four joint coding/modulation schemes considered, namely BICM, TCM3, TCM6, TTCM when communicating over the COST 207 channel of [28].

schemes are of similar complexity, but the TCM3 scheme exhibits a better video performance.

C. Effect of Various AQAM Thresholds

In the previous sections, we have studied the performance of AQAM using the switching thresholds of the “normal” scenario. By contrast, in this section we will study the performance of the TTCM-aided AQAM scheme using the switching thresholds of the “conservative,” “normal,” and “aggressive” scenarios, which were characterized earlier in Table IV. Again, the “conservative,” “normal” and “aggressive” thresholds sets result in a target PLR of 0.5%, 3%, and 20%, respectively.

The three sets of thresholds allowed us to demonstrate, how the performance of the AQAM modem was affected, when the modem used the radio channel more “aggressively” or more “conservatively.” This translated in a more and less frequent employment of the higher throughput, but more error-prone AQAM modes, respectively. Explicitly, the more aggressive switching thresholds provide a higher effective throughput at a cost of a higher PLR. The PSNR versus channel SNR performance of the three AQAM modem switching thresholds is depicted in Fig. 10, where it is shown that the average PSNR of the AQAM modem employing “aggressive” and “normal” switching thresholds is about 4 and 2 dB better than that employing “conservative” switching thresholds, respectively, for channel SNRs ranging from 12 to 30 dB. However, in perceptual video quality terms the best compromise was associated with the “normal” switching threshold set. This was, because the excessive PLR of the “aggressive” set inflicted noticeable channel-induced video degradations, despite the favorable video quality of the unimpaired high-throughput video packets.

V. TTCM AQAM IN CDMA SYSTEM

We have demonstrated that the adaptive video system aided by TTCM performs better than that aided by TCC [22], TCM,

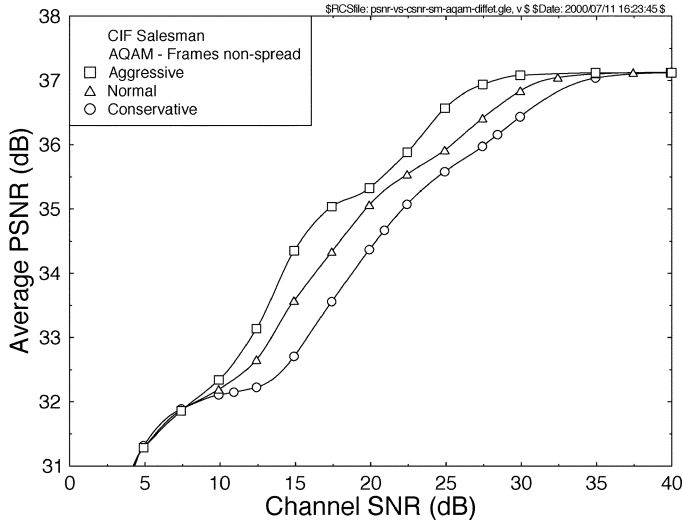


Fig. 10. Average PSNR video quality versus channel SNR for the quadruple-mode TCM AQAM scheme using the three different sets of switching thresholds from Table IV. TCM scheme using a code memory of $M = 3$ and $t = 4$ iterations was used when communicating over the COST 207 channel of [28].

and BICM in a single user scenario. We will now study the performance of the most promising TCM AQAM scheme in the context of direct sequence CDMA (DS-CDMA), when communicating over the UTRA wide-band vehicular Rayleigh fading channels [25] and supporting multiple users.¹

In order to mitigate the effects of multiple access interference (MAI) and ISI, while at the same time improving the systems performance by benefiting from the multipath diversity effects of the channels, we employ the MMSE-based block DFE (MMSE-BDFE) for JD [32] in our system. The multiuser JD-MMSE-BDFE receivers are derivatives of the single-user MMSE-DFE [9], [32], where the MAI is equalized as if it was another source of ISI. The interested readers are referred to [9], [32] for a detailed description of the JD-MMSE-BDFE scheme.

In joint detection systems the signal-to-interference plus noise ratio (SINR) of each user recorded at the output of the JD-MMSE-BDFE can be calculated by using the channel estimates and the spreading sequences of all the users. By assuming that the transmitted data symbols and the noise samples are uncorrelated, the expression used for calculating the SINR γ_o of the n th symbol transmitted by the k th user was given by Klein *et al.* [33] as

$$\gamma_o(j) = \frac{\text{Wanted Signal Power}}{\text{Res. MAI and ISI Power} + \text{Eff. Noise Power}} = \frac{g_j^2 [\mathbf{D}]_{j,j}^2 - 1}{g_j^2 [\mathbf{D}]_{j,j}^2 - 1}, \quad \text{for } j = n + N(k-1) \quad (4)$$

where SINR is the ratio of the wanted signal power to the residual MAI and ISI power plus the effective noise power. The number of users in the system is K and each user transmits N symbols per transmission burst. The matrix \mathbf{D} is a diagonal matrix that is obtained with the aid of the Cholesky decomposition [34] of the matrix used for linear MMSE equalization of the

¹The significance of this research is that although independent adaptive coding and modulation was standardised for employment in the 3G High Speed Data Packet Access mode, this was only proposed for high-latency data transmission. By contrast, here we employ joint adaptive CM in a low-latency, real-time video context.

TABLE V
MODULATION AND CHANNEL PARAMETERS FOR CDMA SYSTEM

Parameter	Value
Carrier Frequency	1.9GHz
Vehicular Speed	30mph
Doppler frequency	85Hz
System Baud rate	3.84 MBd
Normalised Doppler frequency	$85/(3.84 \times 10^6) = 2.21 \times 10^{-5}$
Channel type	UMTS Vehicular Channel A [25]
Number of paths in channel	6
Data modulation	Adaptive Coded Modulation (4QAM, 8PSK, 16QAM, 64QAM)
Receiver type	JD-MMSE-BDFE
No. of symbols per JD block	20

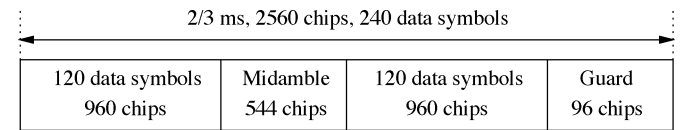


Fig. 11. Modified UTRA burst 1 [24] with a spreading factor of 8. The original UTRA burst has 244 data symbols.

CDMA system [32], [33]. The notation $[\mathbf{D}]_{j,j}^2$ represents the element in the j th row and j th column of the matrix \mathbf{D} and the value g_j is the amplitude of the j th symbol. The AQAM mode switching mechanism used for the JD-MMSE-BDFE of user k is the same as that of (3), where γ_{DFE} of user k was used as the modulation switching metric, which can be computed from

$$\gamma_{DFE}(k) = \frac{1}{N} \sum_{n=1}^N \gamma_o(j), \quad j = n + N(k-1). \quad (5)$$

Again, the log-domain branch metric is computed for the CM trellis decoding scheme using the MMSE-BDFEs symbol estimate by invoking (2).

The UTRA channel model and system parameters of the AQAM CDMA scheme are outlined as follows. Table V shows the modulation and channel parameters employed. The multipath channel model is characterized by its discretized chip-spaced UTRA vehicular channel A [25]. The transmission burst structure of the modified UTRA Burst 1 [24] using a spreading factor of eight is shown in Fig. 11. The number of data symbols per JD block is 20, Hence, the original UTRA Burst 1 was modified to host a burst of 240 data symbols, which is a multiple of 20.

The remaining system parameters are shown in Table VI, where there are 15 time slots in one UTRA frame and we assign one slot for one group of CDMA users. More specifically, each CDMA user group employed a similar system configuration, but communicated with the base station employing another one of the 15 different time slots. In general, the total number of users supportable by the uplink CDMA system can be increased by using a higher spreading factor at the cost of a reduced throughput, since the systems chip rate was fixed at

TABLE VI
GENERIC SYSTEM FEATURES OF THE RECONFIGURABLE MULTI-MODE VIDEO
TRANSCIVER, USING THE SPREAD DATA BURST 1 OF UTRA [24],
[25] SHOWN IN FIG. 11

Features	Value
Multiple access	CDMA, TDD
No. of Slots/Frame	15
Spreading factor, Q	8
Frame length	10ms
Slot length	2/3ms
Data Symbols/Slot/User	240
No. of Slot/User group	1
User Data Symbol Rate (kBd)	240/10 = 24
System Data Symbol Rate (kBd)	24x15 = 360
Chips/Slot	2560
Chips/Frame	2560x15=38400
User Chip Rate (kBd)	2560/10 = 256
System Chip Rate (MBd)	38.4/10 = 3.84
System Bandwidth (MHz)	3.84 x 3/2 = 5.76
Eff. User Bandwidth (kHz)	5760/15 = 384

3.84×10^6 chip/s, as shown in Table V. Another option for increasing the number of users supported is by assigning more uplink time slots for new groups of users. In our study, we investigate the proposed system using one time slot only. Hence, the data symbol rate per slot per user is 24 kBd for a spreading factor of eight. Finally, Table VII shows the operational-mode specific video transceiver parameters for the TTCM AQAM video system, where the effective video bit rate of each user is ranging from 19.8 to 113.8 kb/s. Since the video bit rate is relatively low as a consequence of CDMA spreading, we transmitted 176×144 pixel QCIF resolution video sequences at 30 frames/s based on the H.263 video codec [24].

A. Performance of TTCM AQAM in CDMA System

The PLR and video bit rate performance of the TTCM AQAM CDMA scheme designed for a target PLR of 5% and for supporting $K = 2$ and 4 users is shown in Fig. 12. The PLR was below the target value of 5% and the video bit rate improved, as the channel SNR increased. Since we employed switching thresholds which are constant over the SNR range, in the region of SNR = 10 dB the PLR followed the trend of 4QAM. Similarly, for SNRs between 17 and 20 dB the PLR-trend of 16QAM was predominantly obeyed. In both of these SNR regions a significantly lower PLR was achieved than the target value. We note, however that it is possible to increase the PLR to the value of the target PLR, in this SNR region for the sake of attaining extra throughput gains by employing a set of switching thresholds, where the thresholds are varied as a function of the SNR [35], but this design option was set aside for further research.

TABLE VII
OPERATIONAL-MODE SPECIFIC TRANSCIVER PARAMETERS FOR
TTCM IN CDMA SYSTEM

Features	Multi-rate System			
	4QAM	8PSK	16QAM	64QAM
Mode	4QAM	8PSK	16QAM	64QAM
Transmission Symbols	240			
Bits/Symbol	2	3	4	6
Transmission bits	480	720	960	1440
Packet Rate	100/s			
Transmission bitrate (kbit/s)	48	72	96	144
Code Termination Symbols	6			
Data Symbols	234			
Coding Rate	1/2	2/3	3/4	5/6
Information Bits/Symbol	1	2	3	5
Unprotected bits	234	468	708	1170
Unprotected bitrate (kbit/s)	23.4	46.8	70.8	117.0
Video packet CRC (bits)	16			
Feedback protection (bits)	9			
Video packet header (bits)	11	12	12	13
Video bits/packet	198	431	671	1138
Effective Video-rate (kbit/s)	19.8	43.1	67.1	113.8
Video framerate (Hz)	30			

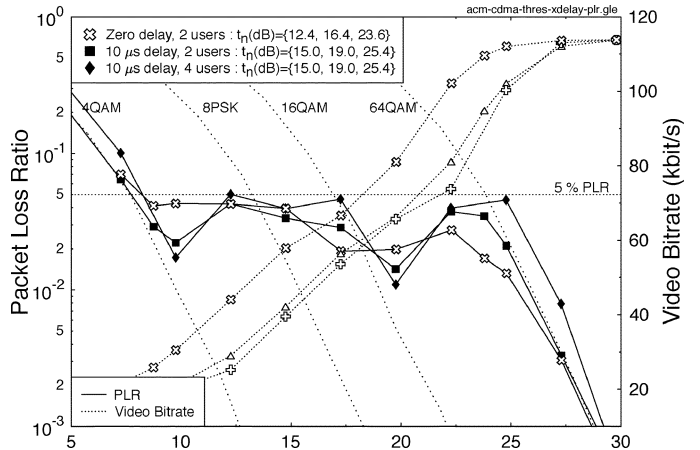


Fig. 12. PLR and video bit rate versus channel SNR for the four fixed TTCM modes and for the quadruple-mode TTCM AQAM CDMA scheme supporting two and four users transmitting the QCIF video sequence at 30 frame/s, when communicating over the UTRA vehicular channel A [25].

From Fig. 12, we also notice that the performance difference between the $K = 2$ and 4 user scenarios is only marginal with the advent of the powerful JD-MMSE-BDFE scheme. Specifically, there was only about one decibel SNR penalty, when the number of users increased from two to four for the 4QAM and 64QAM modes at both low and high SNRs, respectively. The PLR of the system supporting $K = 4$ users was still below the target PLR, when the switching thresholds derived for $K = 2$ users were employed. In terms of the video bit rate performance, the SNR penalty is less than one dB, when the number of users

supported is increased from $K=2$ to 4 users. Note that the delay spread of the chip-spaced UTRA vehicular channel A [25] is $2.51 \mu\text{s}$ corresponding to $2.51 \times 3.84 \approx 10$ chip duration for the 3.84 MBd Baud rate of our system, as seen in Table V. Hence, the delay spread is longer than the spreading code length ($Q=8$ chips) used in our system and, therefore, the resultant ISI in the system is significantly higher, than that of the system employing a higher spreading factor, such as $Q > 10$ chips. These findings illustrated the efficiency of the JD-MMSE-BDFE scheme in combating the high ISI and MAI of the system. More importantly, the employment of the JD-MMSE-BDFE scheme in our system allowed us to generalize our results recorded for the $K=2$ users scenario to that of a higher number of users, since the performance penalty associated with supporting more users was found marginal.

Let us also investigate the effect of mode signalling delay on the performance of the TTCM AQAM CDMA scheme in Fig. 12. The performance of the ideal scheme, where the channel quality estimation is perfect without any signalling delay is compared to that of the proposed practical scheme, where the channel quality estimation is imperfect and outdated by the delay of one frame duration of $10 \mu\text{s}$. For a target PLR of 5%, the ideal scheme exhibited a higher video bit rate than the practical scheme. More specifically, at a target PLR of 5%, about 2.5 dB SNR gain is achieved by the ideal scheme in the SNR region spanning from 8 to 27 dB. A channel quality signalling delay of one frame duration certainly represents the worst case scenario. In general, the shorter the signalling delay the better the performance of the adaptive system. Hence, the performance of the zero-delay and one-frame delay schemes represent the lower-bound and upper-bound performance, respectively, for practical adaptive systems, although employing the channel-quality prediction schemes of [26] and [27] would allow us to approximate the perfect channel estimation scenario.

Let us now evaluate the PSNR performance of the proposed practical TTCM AQAM CDMA scheme. For maintaining a target PLR of 5% in conjunction with an adaptive mode signalling delay of one UTRA frame length of 10 ms, the average PSNR versus channel SNR performance of the quadruple-mode TTCM AQAM CDMA scheme is shown in Fig. 13 together with that of the four fixed TTCM modes. As shown in Fig. 13, the video performance of the TTCM AQAM CDMA scheme supporting $K=4$ users degrades gracefully from the average PSNR of 41.5 to 34.2 dB, as the channel SNR degrades from 30 to 5 dB. Hence, an attractive subjective video performance can be obtained in the UTRA environment. Again, the PSNR performance difference between the $K=2$ and 4 scenario is only marginal with the advent of the powerful JD-MMSE-BDFE scheme invoked [32].

VI. CONCLUSIONS

In this contribution, various BbB AQAM TCM, TTCM and BICM based video transceivers have been studied. The near-instantaneously adaptive transceiver is capable of operating in four different modulation modes, namely 4QAM, 8PSK, 16QAM, and 64QAM.

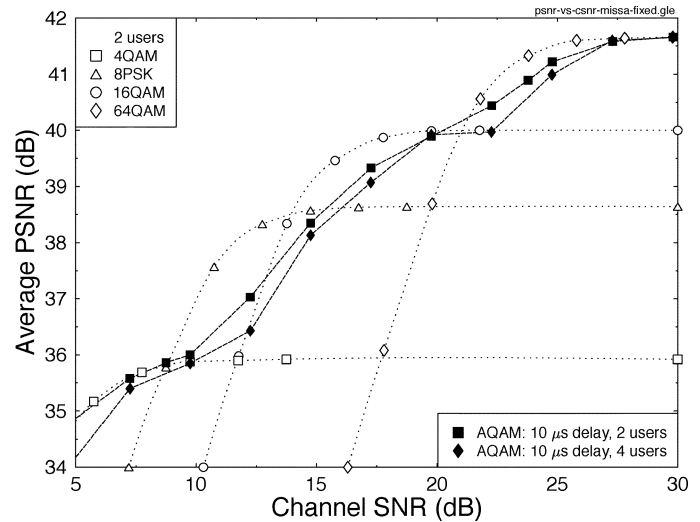


Fig. 13. Average PSNR versus channel SNR for the four fixed TTCM modes and for the quadruple-mode TTCM AQAM CDMA scheme supporting two and four users transmitting the QCIF video sequence at 30 frame/s, when communicating over the UTRA vehicular channel A [25].

The advantage of using CM schemes in our near-instantaneously adaptive transceivers is that when invoking higher order modulation modes in case of encountering a higher channel quality, the coding rate approaches unity. This allows us to maintain as high a throughput as possible. We found that the TTCM scheme provided the best overall video performance due to its superior PLR performance. However, the lower complexity TCM3 assisted scheme provides the best compromise in terms of the PSNR performance and complexity in comparison to the TTCM, TCM6 and BICM assisted schemes.

The BbB AQAM modem guaranteed the same video performance as the lowest and highest order fixed-mode modulation schemes at extremely low and high channel SNRs with a minimal latency. Furthermore, in between these extreme SNRs the effective video bit rate smoothly increased, as the channel SNR increased, whilst maintaining a near-constant PLR. By controlling the AQAM switching thresholds, a near-constant PLR can be maintained. We have also compared the performance of the proposed TTCM AQAM scheme to that of the TCC AQAM arrangement characterized in [22] under similar conditions and the TTCM scheme was found to be more advantageous than the TCC scheme of [22] in the context of the adaptive H.263 video system. The best TTCM AQAM arrangement was also studied in the context of a DS-CDMA system by utilising a JD-MMSE-BDFE scheme and promising results were obtained when communicating in the UTRA environment. It was also apparent from this study that, as long as the DFE or the JD-MMSE-BDFE scheme is capable of transforming the wide-band Rayleigh fading channels error statistics into "AWGN-like" error statistics, the performance trends of the CM schemes observed in AWGN channels will be preserved in the wide-band Rayleigh fading channels. Specifically, the TTCM assisted scheme, which is the best performer when communicating over AWGN channels, is also the best performer when communicating over the wide-band Rayleigh fading channels, when compared to the schemes assisted by TCC, TCM, and BICM. Hence, it is shown that by adapting the video rate, channel coding rate

and the modulation mode together according to the channel quality, the best possible source-signal representation quality is achieved efficiently in terms of bandwidth and power, on a near-instantaneous basis.

Our future research is focused on employing a similar BbB AQAM philosophy in the context of CDMA systems in conjunction with low density parity check CM and the MPEG4 video codec.

REFERENCES

- [1] G. Ungerböck, "Channel coding with multilevel/phase signals," *IEEE Trans. Inf. Theory*, vol. IT-28, no. 1, pp. 55–67, Jan. 1982.
- [2] E. Zehavi, "8-PSK trellis codes for a Rayleigh fading channel," *IEEE Trans. Commun.*, vol. 40, no. 5, pp. 873–883, May 1992.
- [3] G. Caire, G. Taricco, and E. Biglieri, "Bit-interleaved coded modulation," *IEEE Trans. Inf. Theory*, vol. 44, no. 5, pp. 927–946, May 1998.
- [4] C. Berrou, A. Glavieux, and P. Thitimajshima, "Near Shannon limit error-correcting coding and decoding: turbo codes," in *Proc. Int. Conf. Commun.*, Geneva, Switzerland, May 1993, pp. 1064–1070.
- [5] S. L. Goff, A. Glavieux, and C. Berrou, "Turbo-Codes and high spectral efficiency modulation," in *Proc. IEEE Int. Conf. Commun.*, 1994, pp. 645–649.
- [6] P. Robertson and T. Worz, "Bandwidth efficient turbo trellis-coded modulation using punctured component codes," *IEEE J. Sel. Areas Commun.*, vol. 16, pp. 206–218, Feb. 1998.
- [7] U. Wachsmann and J. Huber, "Power and bandwidth efficient digital communications using turbo codes in multilevel codes," *Eur. Trans. Telecommun.*, vol. 6, pp. 557–567, Sep./Oct. 1995.
- [8] D. J. Costello, A. Banarjee, T. E. Fuja, and P. C. Massey, "Some reflections on the design of bandwidth efficient turbo codes," in *Proc. 4th ITG Conf. Source Channel Coding*, Jan. 2002, pp. 357–363.
- [9] L. Hanzo, C. H. Wong, and M. S. Yee, *Adaptive Wireless Transceivers: Turbo-Coded, Turbo-Equalized and Space-Time Coded TDMA, CDMA and OFDM Systems*. New York: Wiley, 2000.
- [10] J. M. Torrancia and L. Hanzo, "Latency and networking aspects of adaptive modems over slow indoors Rayleigh fading channels," *IEEE Trans. Vehic. Technol.*, vol. 48, no. 4, pp. 1237–1251, Apr. 1998.
- [11] J. Torrancia, L. Hanzo, and T. Keller, "Interference aspects of adaptive modems over slow Rayleigh fading channels," *IEEE Trans. Vehic. Technol.*, vol. 48, no. 9, pp. 1527–1545, Sep. 1999.
- [12] A. J. Goldsmith and S. Chua, "Variable-rate variable-power MQAM for fading channels," *IEEE Trans. Commun.*, vol. 45, no. 10, pp. 1218–1230, Oct. 1997.
- [13] C. Wong and L. Hanzo, "Upper-bound performance of a wide-band burst-by-burst adaptive modem," *IEEE Trans. Commun.*, vol. 48, no. 3, pp. 367–369, Mar. 2000.
- [14] S. M. Alamouti and S. Kallel, "Adaptive trellis-coded multiple-phased-shift keying Rayleigh fading channels," *IEEE Trans. Commun.*, vol. 42, no. 6, pp. 2305–2341, Jun. 1994.
- [15] K. J. Hole, H. Holm, and G. E. Oien, "Adaptive multidimensional coded modulation over flat fading channels," *IEEE J. Sel. Areas Commun.*, vol. 18, no. 4, pp. 1153–1158, Jul. 2000.
- [16] A. J. Goldsmith and S. Chua, "Adaptive coded modulation for fading channels," *IEEE Trans. Commun.*, vol. 46, no. 5, pp. 595–602, May 1998.
- [17] D. Goeckel, "Adaptive coding for fading channels using outdated fading estimates," *IEEE Trans. Commun.*, vol. 47, no. 6, pp. 844–855, Jun. 1999.
- [18] V. K. N. Lau and M. D. Macleod, "Variable-rate adaptive trellis coded QAM for flat-fading channels," *IEEE Trans. Commun.*, vol. 49, no. 9, pp. 1550–1560, Sep. 2001.
- [19] P. Ormeci, X. Liu, D. Goeckel, and R. Wesel, "Adaptive bit-interleaved coded modulation," *IEEE Trans. Commun.*, vol. 49, no. 9, pp. 1572–1581, Sep. 2001.
- [20] V. K. N. Lau, "Performance analysis of variable rate: Symbol-by-symbol adaptive bit interleaved coded modulation for rayleigh fading channels," *IEEE Trans. Vehic. Technol.*, vol. 51, no. 5, pp. 537–550, May 2002.
- [21] S. X. Ng, C. H. Wong, and L. Hanzo, "Burst-by-burst adaptive decision feedback equalized TCM, TTCM, BICM and BICM-ID," in *Proc. Int. Conf. Commun.*, Jun. 2001, pp. 3031–3035.
- [22] P. Cherriman, C. Wong, and L. Hanzo, "Turbo- and BCH-coded wide-band burst-by-burst adaptive H.263-assisted wireless video telephony," *IEEE Trans. Circuits Syst. Video Technol.*, vol. 10, no. 12, pp. 1355–1363, Dec. 2000.
- [23] P. Cherriman and L. Hanzo, "Programmable H.263-based wireless video transceivers for interference-limited environments," *IEEE Trans. Circuits Syst. Video Technol.*, vol. 8, no. 6, pp. 275–286, Jun. 1998.
- [24] L. Hanzo, P. Cherriman, and J. Streitz, *Wireless Video Communications: From Second to Third Generation Systems, WLANs and Beyond*. Piscataway, NJ: IEEE Press, 2001.
- [25] "UMTS: Selection Procedures for the Choice of Radio Transmission Technologies of the UMTS," European Telecommunications Standard Institute (ETSI), Paris, France, Tech. Rep. TR101 112 v3.2.0., 1998.
- [26] A. Duel-Hallen, S. Hu, and H. Hallen, "Long range prediction of fading signals," *IEEE Signal Process. Mag.*, vol. 17, pp. 62–75, May 2000.
- [27] L. Hanzo, M. Münster, B. J. Choi, and T. Keller, *OFDM and MC-CDMA for Broadcasting Multi-User Communications, WLANs and Broadcasting*. New York: Wiley, 2003.
- [28] "COST 207: Digital land mobile radio communications, Final Report," Office for Official Publications of the European Communities, Luxembourg, Germany, 1989.
- [29] A. Klein, R. Pirhonen, J. Skoeld, and R. Suoranta, "FRAMES multiple access mode 1—wide-band TDMA with and without spreading," in *Proc. IEEE Int. Symp. Personal, Indoor, Mobile Radio Commun.*, vol. 1, Helsinki, Finland, Sep. 1997, pp. 37–41.
- [30] L. Hanzo, T. H. Liew, and B. L. Yeap, *Turbo Coding, Turbo Equalization and Space Time Coding for Transmission Over Wireless Channels*. New York: Wiley, 2002.
- [31] P. Robertson, E. Villebrun, and P. Höher, "A comparison of optimal and sub-optimal MAP decoding algorithms operating in the log domain," in *Proc. Int. Conf. Commun.*, Jun. 1995, pp. 1009–1013.
- [32] L. Hanzo, L.-L. Yang, E. L. Kuan, and K. Yen, *Single- and Multi-Carrier CDMA*. New York: Wiley, 2003.
- [33] A. Klein, G. Kaleh, and P. Baier, "Zero forcing and minimum mean square error equalization for multiuser detection in code division multiple access channels," *IEEE Trans. Veh. Technol.*, vol. 45, no. 5, pp. 276–287, May 1996.
- [34] G. Golub and C. van Loan, *Matrix Computations*. Baltimore, MD: North Oxford Academic, 1983.
- [35] B. J. Choi and L. Hanzo, "Optimum mode-switching-assisted constant-power single- and multicarrier adaptive modulation," *IEEE Trans. Vehic. Technol.*, vol. 52, no. 5, pp. 536–560, May 2003.



Soon Xin Ng (M'03) received the B.Eng. degree (first-class hon.) in electronics engineering and the Ph.D. degree in mobile communications from the University of Southampton, Southampton, U.K., in 1999 and 2002, respectively.

Currently, he is continuing his research as a Postdoctoral Research Fellow at the University of Southampton. His research interests are mainly in adaptive coded modulation, channel coding, turbo coding, space-time coding, joint source and channel coding, and MIMO systems. He has published

numerous papers in this field.

J. Y. Chung received the B.Eng. degree (first-class hon.) in electrical and electronics engineering from the University of Sussex, Sussex, U.K., in 1998, and the Ph.D. degree in mobile communications from the University of Southampton, Southampton, U.K., in 2004. During his Ph.D. work, he published about a dozen papers.

Currently, he is working for Frontier Silicon Ltd., Cambridge, U.K. His research interests are in the area of error resilient video compression methods, joint source and channel coding, adaptive modulation, channel coding and space-time coding, also encompassing digital multimedia broadcasting (T-DMB), and digital radio broadcasting (DAB).



Peter Cherriman received the M.Eng. degree in information engineering and the Ph.D. degree in mobile video networking from the Department of Electronics and Computer Science, University of Southampton, Southampton, U.K., in 1994, and 1997, respectively.

Following completion of his Ph.D., he is worked on projects for the Mobile Virtual Centre of Excellence, U.K. Currently, he is working for the BBC and his areas of research include robust video coding, microcellular radio systems, power control, dynamic channel allocation, and multiple access protocols.



Lajos Hanzo (M'87–SM'90–F'03) received the M.S. degree in electronics in 1976 and the Ph.D. degree in 1983 from the Technical University of Budapest, Budapest, Hungary. He received the D.Sc. degree from the University Southampton, Southampton, U.K., in 2004.

During his 30-year career in telecommunications, he has held various research and academic posts in Hungary, Germany, and the U.K. Since 1986, he has been with the Department of Electronics and Computer Science, University of Southampton, where he holds the Chair in Telecommunications. He has co-authored 11 books totalling about 9000 pages on mobile radio communications, published in excess of 600 research papers, organized and chaired conference sessions, presented overview lectures, and has been awarded a number of distinctions. He is a nonexecutive Director of the Virtual Centre of Excellence (VCE), U.K., and an enthusiastic supporter of industrial-academic liaison.

Dr. Hanzo is also an IEEE Distinguished Lecturer of both the Communications Society and the IEEE Vehicular Technology (VT) Society. He is a Governor of the IEEE VT society and an Editor for the PROCEEDINGS OF THE IEEE. He is a Fellow of and Institute of Electronics Engineers, U.K. and the Royal Academy of Engineering.